Biosensors and Bioelectronics 25 (2010) 1370–1375

Contents lists available at ScienceDirect

Biosensors and Bioelectronics

journal homepage: www.elsevier.com/locate/bios

Covalent coupling of organophosphorus hydrolase loaded quantum dots to carbon nanotube/Au nanocomposite for enhanced detection of methyl parathion

Dan Du[a,b,*], Wenjuan Chen[a], Weiying Zhang[a], Deli Liu[a], Haibing Li[a], Yuehe Lin[b,**]

[a] Key Laboratory of Pesticide and Chemical Biology of Ministry of Education, College of Chemistry, Central China Normal University, Wuhan 430079, PR China
[b] Pacific Northwest National Laboratory, Richland, WA 99352, USA

ARTICLE INFO

Article history:
Received 7 August 2009
Received in revised form 21 October 2009
Accepted 21 October 2009
Available online 30 October 2009

Keywords:
Multiwalled carbon nanotube
CdTe quantum dots
Methyl parathion degrading enzyme
Methyl parathion
Amplification

ABSTRACT

An amperometric biosensor for highly selective and sensitive determination of methyl parathion (MP) was developed based on dual-signal amplification: (1) a large amount of introduced enzyme on the electrode surface and (2) synergistic effects of nanoparticles towards enzymatic catalysis. The fabrication process includes (1) electrochemical deposition of gold nanoparticles by a multi-potential step technique at multiwalled carbon nanotube (MWCNT) film pre-cast on a glassy carbon electrode and (2) immobilization of methyl parathion degrading enzyme (MPDE) onto a modified electrode through CdTe quantum dots (CdTe QDs) covalent attachment. The introduced MWCNT and gold nanoparticles significantly increased the surface area and exhibited synergistic effects towards enzymatic catalysis. CdTe QDs are further used as carriers to load a large amount of enzyme. As a result of these two important enhancement factors, the proposed biosensor exhibited extremely sensitive, perfectly selective, and rapid response to methyl parathion in the absence of a mediator. The detection limit was 1.0 ng/mL. Moreover, since MPDE hydrolyzes pesticides containing the P–S bond, it showed high selectivity for detecting MP and many interfering compounds, such as carbamate pesticides. Other organophosphorous pesticides and oxygen-containing inorganic ions (SO_4^{2-}, NO_3^-) did not interfere with the determination. The proposed MPDE biosensor presents good reproducibility and stability, and the MPDE is not poisoned by organophosphate pesticides. Unlike cholinesterase-based biosensor, the MPDE biosensor can be potentially reused and is suitable for continuous monitoring.

1. Introduction

Organophosphates (OPs) have been widely used as pesticides in the agricultural industry and as chemical warfare agents (Giordano and Collins, 2007; Hendrickson and Hedges, 2005; Young et al., 2004). The acute toxicity of an exposure to these OP chemicals stems from the fact that they target a number of important proteins, including a group of hydrolytic enzymes, such as acetylcholinesterase (AChE), which is particularly critical for central and peripheral nervous-system functions (Du et al., 2007; Wang et al., 2009). Chemo/biosensors offer a simple and inexpensive approach for rapid and onsite monitoring of OP exposure (Lin et al., 2004; Liu and Lin, 2006). However, most biosensors for OPs are based on determining the uninhibited AChE activity (Du et al., 2008, 2009; Huang et al., 2008). Such inhibition biosensors are not selective to OPs since AChE is also the target of carbamate pesticide.

A growing class of bacterial enzymes known as phosphotriesterases has recently been characterized. Unlike AChE, these enzymes catalyze the hydrolysis of OPs with a high turnover rate. The typical one is organophosphorus hydrolase (OPH), which exhibits the capability to hydrolyze a large variety of OP compounds by producing less toxic products, such as *p*-nitrophenol and diethyl phosphate (Bird et al., 2008; Karnati et al., 2007). Biosensors based on a catalytic reaction are superior to the inhibition mode since they can be potentially reused and are also suitable for continuous monitoring (Wang et al., 2003). Several types of OPH-based amperometric, potentiometric, or optical biosensors have been described (Mulchandani et al., 1999; Viveros et al., 2006). Methyl parathion degrading enzyme (MPDE) is one kind of OPH. It can detect methyl parathion (MP), which is an extensively used OP pesticide, with high selectivity since MPDE hydrolyzes the P–S bond containing agent. MPDE catalyzes the hydrolysis of MP to generate an equimolar amount of *p*-nitrophenol, which, in turn, is electrochemically oxidized at the working electrode poised at a fixed potential to generate a current that is proportional to the pesticide concentra-

* Corresponding author at: Key Laboratory of Pesticide and Chemical Biology of Ministry of Education, College of Chemistry, Central China Normal University, Luoyu Road 2, Wuhan 430079, Hubei Province, PR China.
** Corresponding author.
E-mail addresses: dudan@mail.ccnu.edu.cn (D. Du), yuehe.lin@pnl.gov (Y. Lin).

0956-5663/$ – see front matter © 2009 Elsevier B.V. All rights reserved.
doi:10.1016/j.bios.2009.10.032

tion. The sensitivity of the electrochemical signal can be further enhanced by using various nanomaterial-based amplifications and can lead to ultrasensitive bioassays (Daniel and Astruc, 2004; Wang, 2005). Two approaches have been developed for nanoparticle-based electrochemical biosensors: (1) nanoparticles are directly used as an electroactive reporter and (2) nanoparticles are used as carriers to load a large amount of electroactive species, e.g., ferrocene, as reporters/markers for amplifying the detection of biomolecules (Wang and Lin, 2008).

Here, we introduced gold nanoparticles by a multi-potential step technique with carbon nanotubes (CNTs) pre-cast on a glassy carbon electrode (GCE) to immobilize MPDE through a CdTe quantum dots (CdTe QDs) covalent attachment. It is easy to electrodeposit gold nanoparticles, and the layer thickness can be controlled. The introduced CNTs and gold nanoparticles significantly increased the surface area and exhibited synergistic effects towards enzymatic catalysis. CdTe QDs are further used as carriers to load a large amount of enzyme. Since MPDE is not poisoned by OP pesticides, it can be potentially reused and is suitable for continuous monitoring. As a result of the dual-signal amplification and high selectivity, the proposed pesticide exhibits extremely sensitive, perfectly selective, and rapid response to MP in the absence of a mediator.

2. Experimental

2.1. Reagents

The positive clone's individual bacterial strain was purchased from Ovagen (Darmstadt, Germany). All bacterial strains were cultured in liquid or on an LB plate at 37 °C. Enzymes and reagents for enzyme manipulation and expression were purchased from New England Biolabs (Beverly, MA), Promega (Madison, WI), and Sigma (St. Louis, USA). MP, cysteamine, *N*-hydroxysuccinimide (NHS), and 1-ethyl-3-(3-dimethylaminopropyl) carbodiimide hydrochloride (EDC) were purchased from Sigma–Aldrich (St. Louis, USA) and used as received. The powder and the thioglycolic acid (TGA) were purchased from Acros Organics (Geel, Belgium). Gold(III) chloride hydrate (3.9 g/mL) was purchased from Treechem Co. (Shanghai, China). Multiwalled carbon nanotubes (MWCNTs) were purchased from Shenzhen Nanotech Port Co., Ltd., China. *N,N*-Dimethylformamide (DMF), $CdCl_2$, $NaBH_4$, phosphate buffer saline (PBS), and other reagents used were of analytical reagent grade. All solutions were prepared using double distilled water.

The colonies were plated on a Luria–Bertani medium containing kanamycin and incubated at 37 °C and 150 rpm for 12 h. The ligation mixture was then transformed into a 250-mL Luria–Bertani medium containing kanamycin and incubated at 37 °C until the OD_{600} was 0.6–0.8. The cultures were plated on a Luria–Bertani medium containing isopropyl-β-D-1-thiogalactopyranoside and incubated at 37 °C for 6 h. The media were collected and centrifuged with 8000 rpm for 5 min at 4 °C to remove any cellular residue. The cells were washed with Tris–Cl buffer (50 mM, pH 8.0) and lysed with lysozyme at 37 °C for 30 min. The final concentration of lysozyme was 100 mg/mL. After ultrasonication for 30 min, the mixtures were centrifuged for 30 min at 4 °C at 12,000 rpm, and the supernatant was MPDE. When evaluating the accurate concentration of MPDE, 10 μL of the MPDE supernatants was added into the mixed solution containing 1.0 mg/mL of 50 μL methyl parathion and 940 μL Tris–Cl buffer (50 mM, pH 8.0) and incubated at 37 °C for 10 min. Then 0.5 mL 10% acetocaustin was added to terminate the reaction. In order to determinate the *p*-nitrophenol and enzyme activity, 0.5 mL of 10% Na_2CO_3 was transformed into the above mixture and detected at OD_{405}. The final concentration of MPDE was 1.0 mg/mL.

2.2. Instrumentation

The electrochemical measurements were carried out on a CHI 660c electrochemical working station (CH Instruments Co., Shanghai, China). A three-electrode system was employed with the modified glassy carbon electrode as the working electrode, a saturated calomel electrode as the reference electrode, and platinum wire as the counter electrode. The electrochemical impedance experiment was carried out in 5 mM $Fe(CN)_6^{4-/3-}$ with frequencies ranging from 100 kHz to 0.1 Hz with an amplitude of 5 mV. Field-emission scanning electron microscopy measurements were performed with a JEOL-6700F (JEOL Ltd., Tokyo, Japan).

2.3. Preparation of CdTe QDs

CdTe QDs were prepared according to the method described elsewhere (Gao et al., 1998). The molar ratio of Cd^{2+}:TGA:HTe^- was fixed at 1:2.5:0.5. Briefly, 0.095 g $CdCl_2{\cdot}2.5H_2O$ was dissolved in 5 mL of water, and 0.092 mL of TGA was added. Next, the solution was adjusted to pH 11 with 1 M NaOH and deaerated with N_2 for 30 min. Next, an oxygen-free NaHTe solution, which was freshly prepared from tellurium powder and $NaBH_4$ in water, was injected into the above solution under vigorous stirring. Finally, the CdTe QDs functionalized with carboxyl groups were dispersed in PBS and its final concentration was 5 mM. The average diameter of CdTe QDs was about 3 nm (Du et al., 2008). The solution was then heated at 60 °C for 2 h. Finally, CdTe QDs were obtained in aqueous media.

2.4. Preparation of QD–MPDE conjugates

QD nanocrystals were activated with 10 mM EDC and NHS, followed by stirring for 30 min. The resulting mixture was centrifuged for 1 min at 5000 rpm to remove the supernatant solution and then re-dispersed in 250 μL PBS. At room temperature, 50 μL MPDE with a concentration of 1.0 mg/mL was added into the above activated QD solution and mixed for 1 h. The resulting QD–MPDE conjugate was collected by centrifugation at 15,000 rpm for 5 min. After removing the supernatant solution, the purified QDs–MPDE conjugates were produced and re-suspended in 500 μL PBS. Finally the concentration of the QD–MPDE conjugates was 100 ng/mL.

2.5. Electrode preparation and MWCNT film formation

GCE was polished to a mirror finish using the BAS-polishing kit with 0.3 and 0.05 μm Al_2O_3 paste. After being sonicated with ethanol and water, the electrode was applied to a potential of +1.75 V under stirring in pH 5.0 PBS for 300 s, and then the electrode was scanned from +0.3 V to +1.25 V and +0.3 V to −1.3 V until a steady-state current–voltage curve was obtained (Du et al., 2005). The MWCNT was refluxed in HNO_3 for 10 h. The pretreated MWCNT (1.2 mg) was then dispersed in dimethylformamide (DMF) solution and sonicated thoroughly until a homogeneous suspension was obtained. About 2 h of sonication was necessary to obtain well-dispersed MWCNT. Then, a 2 mg/mL MWCNT suspension (5 μL) was applied to the GCE surface and dried in the air.

2.6. Electrodeposition of gold nanoparticles on the MWCNT film

Gold nanoparticles were deposited from a 10-mM $HAuCl_4$ solution in 0.5 M H_2SO_4 on the MWCNT-modified GCE by a multi-potential step electrodeposition technique (Hrapovic et al., 2007), using an electrochemical workstation. In brief, a reduction potential (−0.3 V) was applied for a fixed period (1 s), followed by a relaxation potential of 1.3 V for 5 s in repeated cycles. The number of cycles was optimized by comparing the signal response to MP. This procedure could provide stable gold nanoparticles, with

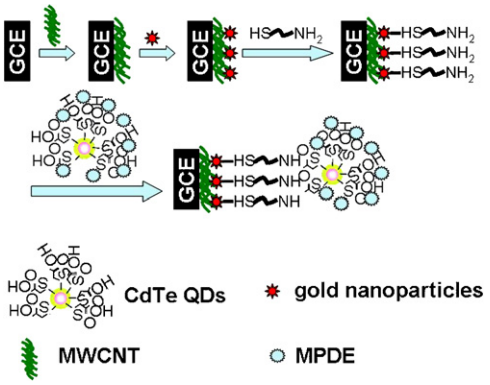

Scheme 1. Preparation procedure for methyl parathion degrading enzyme biosensor.

controllable size and density, allowing a maximum longevity of the electrode.

2.7. Preparation of MPDE biosensor

After rinsing with water, the modified electrode was immersed in 50 mM cysteamine aqueous solution for 8 h at room temperature in darkness to form cysteamine monolayer. Then it was washed thoroughly with double distilled water to remove physically adsorbed cysteamine and soaked in 50 μL QD–MPDE conjugates for 12 h and dried in the air to obtain the MPDE biosensor (MPDE–CdTe/Cys/Au_{nano}/MWCNTs/GCE). Scheme 1 outlined the steps of fabricating processes of the biosensor.

2.8. Amperometric analysis of MP

Amperometric analysis was performed in PBS (pH 7.0) added with different concentrations of methyl parathion. Linear scan voltammograms were performed. The voltammogram was continuously recorded between 0 and 1.0 V at a scan rate of 50 mV/s. All measurements were performed at room temperature. The reaction and transduction scheme exploited for the reported biosensor can be represented by reactions (1) and (2) shown as follows:

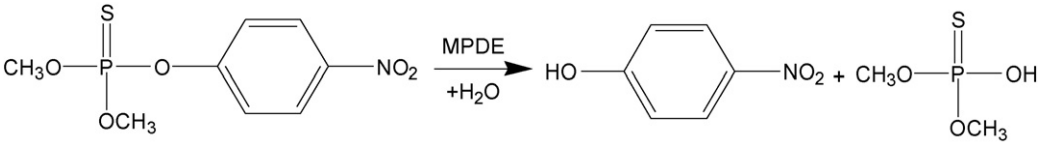

(1)

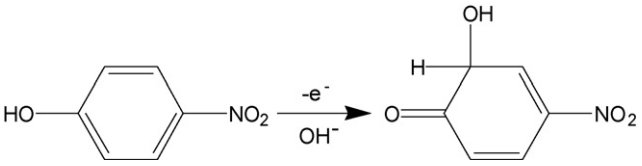

(2)

3. Results and discussion

3.1. Electrodeposition of gold nanoparticles and SEM observation

A two-step potential program was performed on electrodes at different numbers of cycles until an optimal signal towards MP was obtained (Fig. S1, see supporting information). The size and number of gold nanoparticles deposited on the MWCNT during nucleation was affected by gold salt concentration, deposition potential, and the number of deposition cycles. From the scanning electron microscopy (SEM) images of MWCNT and Au_{nano}/MWCNT films (Fig. 1), it can be seen that a network-like structure of MWCNT without aggregation was evenly coated on the surface of the electrode (Fig. 1A). Fig. 1B showed further electrodeposition of gold nanoparticles on the MWCNT film. The high magnification image (Fig. 1C) provided strong evidence for the successful formation of gold nanoparticles on the MWCNT film. The diameter of the MWCNTs (40 nm) and the size of the gold nanoparticles (20 nm) can be observed from Fig. 1C. A non-uniform coating occasionally observed might be attributable to island formation during initial MWCNT coating or possible aggregation following electrodeposition preparation.

3.2. Electrochemical impedance spectroscopy of the biosensor

Electrochemical impedance spectroscopy (EIS) can provide useful information on the impedance changes of the electrode surface during the fabrication process (Park and Yoo, 2003). In EIS, the semicircle diameter equals the electron-transfer resistance, R_{ct}. This resistance controls the electron-transfer kinetics of the redox probe at the electrode interface. Fig. 2 illustrated typical Nyquist plots obtained from bare GCE, MWCNT/GCE, Au_{nano}/MWCNT/GCE, Cys/Au_{nano}/MWCNT/GCE and MPDE-CdTe/Cys/Au_{nano}/MWCNT/GCE using $Fe(CN)_6^{3-/4-}$ as the redox probe. As shown in curve a, the bare GCE presented a semicircle diameter of 150 Ω with an almost straight tail line, indicating the characteristic of a diffuse limiting step of the electrochemical process. An obvious decrease in the R_{ct} (46 Ω) was observed after immobilization of MWCNT on the electrode surface (curve b). Here MWCNT immobilized on the electrode played an important role similar to an electron-conducting tunnel, making electron transfer to the electrode surface easier. When gold nanoparticles were further deposited on the MWCNT film, there was no obvious change in the R_{ct}, and an almost straight line was exhibited (curve c). The interface modified with gold nanoparticles showed a lower R_{ct} compared to that of bare electrode, indicating that their good conductivity of Au_{nano} has a contribution to electron transfer. After a layer of cysteamine assembled on the electrode surface, a slight increase in R_{ct} (230 Ω) at Cys/Au_{nano}/MWCNT/GCE was clearly observed (curve d). The electrodeposited cysteamine increased the impedance of electrode. Then the MPDE–CdTe QDs-immobilized surface showed a great increase in diameter of semicircle due to the increase of the thickness of the interface (curve e), suggesting that enzyme layer formed an additional barrier and further prevented the redox probe to the electrode surface. Since only CdTe QDs layer did not introduce obvious barrier, it was the direct evidence of successful binding of enzyme on the electrode surface.

To understand the synergistic effect of the Au_{nano}–MWCNT composite film, we detail the studies of the electrocatalytic behavior of the film on the electrode toward the oxidation of the electroactive product, *p*-nitrophenol. Control experiments on MWCNT/GCE and Au_{nano}/GCE were also carried out to understand the contribution of individual components and the possible synergistic effects among them. Fig. 3 shows the hydrodynamic voltammograms of Au_{nano}/MWCNT/GCE (curve a), MWCNT/GCE (curve b) and Au_{nano}/GCE (curve c) with *p*-nitrophenol addition. As shown in this figure, the MWCNT/GCE improved the electrocatalytic activity to *p*-nitrophenol compared with that at the Au_{nano}/GCE. Furthermore, the Au_{nano}–MWCNT composite exhibited the highest electrochemical response. The magnitude of the electrochemical

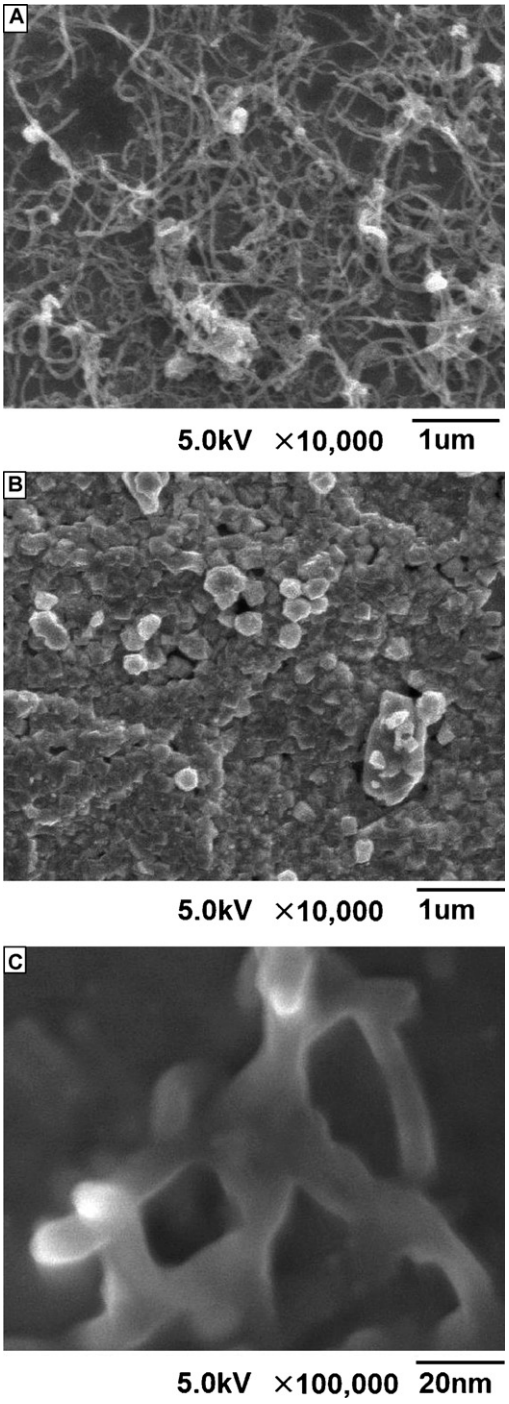

Fig. 1. SEM images of (A) MWCNT, (B) Au_{nano}/MWCNT and (C) magnified Au_{nano}/MWCNT films.

response at these different electrodes increases in the following order: Au_{nano}/MWCNT/GCE > MWCNT/GCE (curve b) > Au_{nano}/GCE. It can be concluded that the nanocomposite film with both gold and MWCNT nanoparticles shows a synergistic effect on the electrocatalytic activity to *p*-nitrophenol. Another issue was related to electrode surface. The difference of the electrode's surface area also influences the magnitude of the electrochemical response. According to Randles–Sevcik equation, the electroactive areas of the Au_{nano}/MWCNT/GCE, MWCNT/GCE, Au_{nano}/GCE and bare GCE were calculated to be 1.29 cm^2, 1.03 cm^2, 1.12 cm^2 and 0.15 cm^2, respectively. Obviously, the artificially modification increased the surface area 8–9-fold comparing with the bare electrode. However the surface areas of the Au_{nano}/MWCNT/GCE, MWCNT/GCE and Au_{nano}/GCE were almost the same. The magnitude of the electrochemical response was attributed to the individual components on the surface. Therefore, the Au_{nano}/MWCNT/GCE exhibited the highest electrocatalytic activity toward *p*-nitrophenol. We did not observe QDs have electrocatalytic activity toward *p*-nitrophenol. QDs used here were served as carrier to load more enzymes, which resulted in further improvement of the sensitivity.

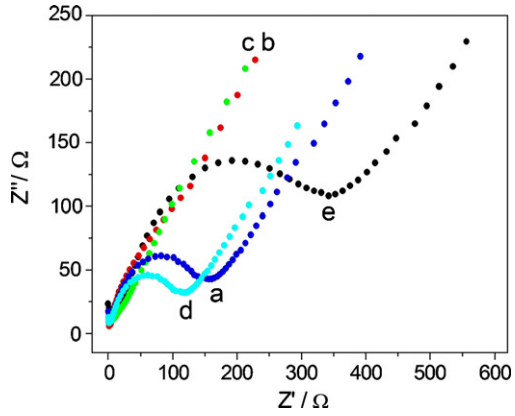

Fig. 2. Electrochemical impedance spectra of (a) bare GCE, (b) MWCNT/GCE, (c) Au_{nano}/MWCNT/GCE, (d) Cys/Au_{nano}/MWCNT/GCE and (e) MPDE–CdTe/Cys/Au_{nano}/MWCNT/GCE recorded in pH 7.0 PBS containing 50 mM $K_3Fe(CN)_6$ and $K_4Fe(CN)_6$.

3.3. Optimization of experimental parameters

The effect of MWCNT concentration on the response current was studied. We found that more MWCNT led to higher signal current, and when its concentration increased to 2 mg/mL, no obvious enhancement of current was observed. Since MWCNT possessed a high surface-to-volume ratio, MWCNT-coated GCE usually has much larger surface areas than bare GCE. The enrichment effect to the analyte could contribute to the increase of the response. Thus, 2 mg/mL MWCNT was selected to prepare the biosensor (see supporting information, Fig. S2A).

The response also changed with the content of electrodeposited gold nanoparticles (see support information, Fig. S2B). The increase of electrodeposition cycles resulted in a slight enhancement of the current signal at first, and then a sharp increase was observed

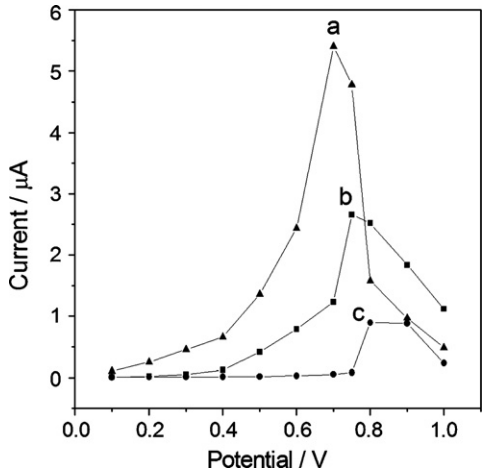

Fig. 3. Hydrodynamic voltammogram of *p*-nitrophenol obtained at (a) Au_{nano}/MWCNT/GCE, (b) MWCNT/GCE and (c) Au_{nano}/GCE. *p*-Nitrophenol was obtained by mixing 1 mg mL^{-1} MPDE with 100 ng mL^{-1} MP for 10 min.

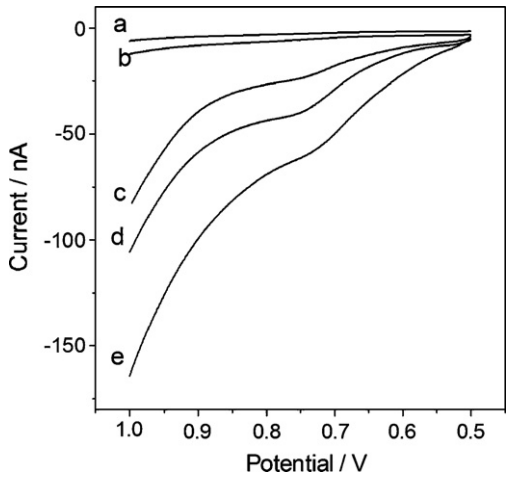

Fig. 4. The linear scan voltammograms of 100 ng mL^{-1} MP at (a) Cys/Au$_{nano}$/MWCNT/GCE, (b) QD/Cys/Au$_{nano}$/MWCNT/GCE, (c) MPDE–CdTe/Cys/Au$_{nano}$/MWCNT/GCE and (d) 200 ng mL^{-1} MP and (e) 400 ng mL^{-1} MP at MPDE–CdTe/Cys/Au$_{nano}$/MWCNT/GCE.

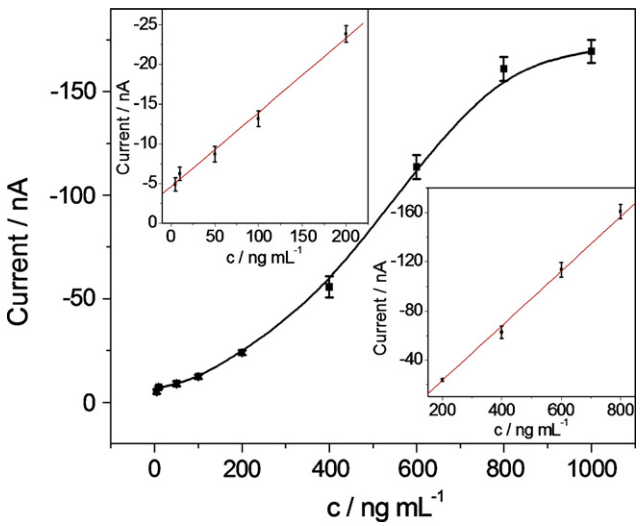

Fig. 5. Response curves for MP in pH 7.0 PBS at MPDE–CdTe/Cys/Au$_{nano}$/MWCNT/GCE. *Inset:* the calibration curves for MP determination.

with further electrodeposition until 12 cycles. The current signal decreased, however, with a continuous scan for electrodeposition. This might be due to congregation of nanoparticles, resulting in a larger size Thus, electrodeposition for 12 cycles was selected to prepare the biosensor.

3.4. Electrochemical response of MP at MPDE–QD/Cys/Au$_{nano}$/MWCNT/GCE

Fig. 4 showed the linear scan voltammograms of MP with different concentrations at electrodes. No apparent peak was observed at Cys/Au$_{nano}$/MWCNT/GCE (curve a) and CdTe/Cys/Au$_{nano}$/MWCNT/GCE (curve b). However, when the MPDE–QD conjugate was coupled to the electrode, the MPDE–CdTe/Cys/Au$_{nano}$/MWCNT/GCE displayed an oxidation peak with E_{pa} = 0.75 V (curve c). Obviously this peak came from the oxidation of *p*-nitrophenol, a hydrolysis product of MP, catalyzed by the immobilized MPDE. The oxidation current increased with increasing MP concentration (curves d and e). The calibration curve under the optimized experimental conditions was shown in Fig. 5. The linear response range of the biosensor to MP concentration was described with two segments. One was from 5.0 ng/mL to 200 ng/mL, and the other one was from 200 ng/mL to 1000 ng/mL with correlation coefficients of 0.994 and 0.996 respectively. The detection limit was 1.0 ng/mL, which is comparable with that reported electrochemical sensor (Gong et al., 2009a,b; Viswanathan et al., 2009). However, these sensors are based on inhibition of cholinesterase activity by OPs or direct electrochemical response of MP. Our MPDE biosensor has the advantage of higher selectivity to OPs containing P–S bond and is suitable for continuous monitoring using a flow system.

Interferences arising from carbamate pesticides, other organophosphorus pesticides and oxygen-containing inorganic ions (SO_4^{2-}, NO_3^-) that are expected to coexist in solution were used to evaluate the selectivity of MPDE–QDs/Cys/Au$_{nano}$/MWCNT/GCE to MP. Separate detection experiments were performed with 100 ng/mL MP in PBS (pH 7.0) solution in the absence and presence of 100 ng/mL of carbaryl, 100 ng/mL dimethoate, 100 ng/mL monocrotophos, 100 ng/mL malathion, 0.1 M of SO_4^{2-} and 0.1 M of NO_3^-. One can see that carbamate pesticides, other OP pesticides and oxygen-containing inorganic ions do not interfere with the detection of MP (see supporting information, Fig. S3). Since MPDE hydrolyzes pesticides containing the P–S bond, it shows high selectivity to MP.

To further demonstrate the practicality of the proposed biosensor, the recovery test was studied by adding different amounts of 100 ng/mL MP into garlic samples of 0.1 M PBS (pH 7.0). The recoveries were from 96.0% to 101.3%. These results indicated that the proposed method was highly accurate, precise and reproducible. It can be used for direct analysis of real samples.

3.5. Precision of measurements and stability of biosensor

Since MPDE is not poisoned by OP pesticides, unlike cholinesterases, the sensor can be potentially reused and are also suitable for continuous monitoring. To prove the precision and practicability of the proposed method, the reproducibility and storage stability of the biosensor were also examined. The intra-assay precision of the biosensors was evaluated by assaying one enzyme electrode for eight replicate determinations in 50 ng/mL MP. Similarly, the inter-assay precision, or fabrication reproducibility, was estimated at eight different electrodes. The relative standard deviation of the intra-assay and inter-assay were found to be 3.0% and 8.7%, respectively, indicating acceptable precision and reproducibility.

When the enzyme electrode was not in use, it was stored at 4 °C in a dry condition. No obvious decrease in the response of methyl parathion was observed in the first 10-day storage. After a 30-day storage period, the sensor retained 90% of its initial current response.

4. Conclusion

We have successfully developed an amperometric biosensor for highly selective and sensitive determination of methyl parathion. A remarkably low detection limit has been achieved through dual-signal amplification offered by the synergistic effects of MWCNT and gold nanoparticles and loading more enzymes through CdTe QDs. The high selectivity of MPDE toward pesticides containing the P–S bond precludes many possible interferences, such as carbamate pesticides, other organophosphorous pesticides, and oxygen-containing inorganic ions. Unlike cholinesterases-based biosensor, the MPDE biosensor is not poisoned by OP pesticides and can be potentially reused and suitable for continuous monitoring.

Acknowledgements

This work is partially supported by the National Natural Science Foundation of China (No. 20705010), the Research Fund for the Doctoral Program of Higher Education of China (No. 20070511015), and a LDRD program at Pacific Northwest National Laboratory (PNNL). PNNL is operated by Battelle for DOE under Contract DE-AC05-76L01830.

Appendix A. Supplementary data

Supplementary data associated with this article can be found, in the online version, at doi:10.1016/j.bios.2009.10.032.

References

Bird, S.B., Sutherland, T.D., Gresham, C., Oakeshott, J., Scott, C., Eddleston, M., 2008. Toxicology 247, 88–92.
Daniel, M.C., Astruc, D., 2004. Chem. Rev. 104, 293–346.
Du, D., Chen, S.Z., Cai, J., Zhang, A.D., 2007. Biosens. Bioelectron. 23, 130–134.
Du, D., Chen, S.Z., Song, D.D., Li, H.B., Chen, X., 2008. Biosens. Bioelectron. 24, 475–479.
Du, D., Chen, W.J., Cai, J., Zhang, J.M., Tu, H.Y., Zhang, A.D., 2009. J. Nanosci. Nanotechnol. 9, 2368–2373.
Du, D., Ju, H.X., Zhang, X.J., Chen, J., Cai, J., Chen, H.Y., 2005. Biochemistry 44, 11539–11545.
Gao, M.Y., Kirstein, S., Mohwald, H., Rogach, A.L., Kornowski, A., Eychmuller, A., Weller, H., 1998. J. Phys. Chem. B 102, 8360–8363.
Giordano, B.C., Collins, G.E., 2007. Curr. Org. Chem. 11, 255–256.
Gong, J.M., Wang, L.Y., Song, D.D., Zhu, X.L., Zhang, L.Z., 2009a. Biosens. Bioelectron. 25, 493–496.
Gong, J.M., Wang, L.Y., Zhang, L.Z., 2009b. Biosens. Bioelectron. 24, 2285–2288.
Hendrickson, R.G., Hedges, J.R., 2005. Crit. Care Clin. 21, 641–652.
Hrapovic, S., Liu, Y., Luong, J.H.T., 2007. Anal. Chem. 79, 500–507.
Huang, X., Du, D., Gong, X.J., Cai, J., Tu, H.Y., Xu, X., Zhang, A.D., 2008. Electroanalysis 20, 402–409.
Karnati, C., Du, H.W., Ji, H.F., Xu, X.H., Lvov, Y., Mulchandani, A., Mulchandani, P., Chen, W., 2007. Biosens. Bioelectron. 22, 2636–2642.
Lin, Y.H., Lu, F., Wang, J., 2004. Electroanalysis 16, 145–149.
Liu, G.D., Lin, Y.H., 2006. Anal. Chem. 78, 835–843.
Mulchandani, A., Mulchandani, P., Chen, W., Wang, J., Chen, L., 1999. Anal. Chem. 71, 2246–2249.
Park, S.M., Yoo, J.S., 2003. Anal. Chem. 75, 455A–461A.
Viveros, L., Paliwal, S., McCrae, D., Wild, J., Simonian, A.A., 2006. Sens. Actuators B 115, 150–157.
Viswanathan, S., Radecka, H., Radecki, J., 2009. Biosens. Bioelectron. 24, 2772–2777.
Wang, H., Wang, J., Choi, D., Tang, Z.W., Wu, H., Lin, Y.H., 2009. Biosens. Bioelectron. 24, 2377–2383.
Wang, J., 2005. Small 1, 1036–1043.
Wang, J., Kraus, R., Block, K., Musameh, M., Mulchandani, A., Schöning, M.J., 2003. Biosens. Bioelectron. 18, 255–260.
Wang, J., Lin, Y.H., 2008. TrAC-Trend. Anal. Chem. 27, 619–626.
Young, S., Balluz, L., Malilay, J., 2004. Sci. Total Environ. 322, 3–20.